

Supporting Information

Lamellar NiMoCo@CuS Enabling Electrocatalytic Activity and Stability for Hydrogen Evolution

Weidong He^a, Wei Wei^a, Bin Wen^a, Dongyi Chen^a, Jiancong Zhang^a, Yue Jiang^{*a},
Guanping Dong^{ab}, Yuying Meng^c, Guofu Zhou^d, Jun-Ming Liu^{ae}, Krzysztof Kempa^{af},
and Jinwei Gao^{*a}

^a Institute for Advanced Materials and Guangdong Provincial Key Laboratory of Optical Information Materials and Technology, South China Academy of Advanced Optoelectronics, South China Normal University, Guangzhou 510006, China.

^b School of Mechanical and Automotive Engineering, South China University of Technology, Guangzhou 510640, China

^c Institute of Advanced Wear & Corrosion Resistant and Functional Materials, Jinan University, 510632, P. R. China

^d Guangdong Provincial Key Laboratory of Optical Information Materials and Technology & Institute of Electronic Paper Displays, South China Academy of Advanced Optoelectronics, South China Normal University, Guangzhou 510006, China.

^e Laboratory of Solid State Microstructures, Nanjing University, Nanjing 210093, China.

^f Department of Physics, Boston College, Chestnut Hill, Massachusetts 02467, USA

Experimental section

Chemical and materials

All the chemicals in this work, including nickel chloride hexahydrate ($\text{NiCl}_2 \cdot 6\text{H}_2\text{O}$, 98%), sodium molybdate dihydrate ($\text{Na}_2\text{MoO}_4 \cdot 2\text{H}_2\text{O}$, 99%), cobalt nitrate hexahydrate ($\text{Co}(\text{NO}_3)_2 \cdot 6\text{H}_2\text{O}$, 97.7%), tetrasodium pyrophosphate decahydrate ($\text{Na}_4\text{P}_2\text{O}_7 \cdot 10\text{H}_2\text{O}$, 99%), sodium bicarbonate (NaHCO_3 , 99.5%), concentrated sulfuric acid (H_2SO_4 , 98%), nickel foam (NF), Hydrazine hydrate ($\text{H}_4\text{N}_2 \cdot \text{H}_2\text{O}$, 99%), copper chloride dihydrate ($\text{CuCl}_2 \cdot 2\text{H}_2\text{O}$, 99%), sodium sulfide (Na_2S , 98%), ethanol ($\text{CH}_3\text{CH}_2\text{OH}$, 99%), acetone (CH_3COCH_3 , 99.5%) were obtained commercially and used without further purification. All the solvents used were of analytical grade. Deionized water (DI water, 18.2 M Ω cm)

Synthesis of NiMo/NF and NiMoCo/NF: NiMo/NF and NiMoCo/NF are both synthesized through electrodeposition. First, the NF (1*1 cm²) is ultrasonically treated in 5 M H_2SO_4 for 5 min in advance, then successively washed with ethanol, acetone and deionized water. 50 mL water solution with 0.4755 g $\text{NiCl}_2 \cdot 6\text{H}_2\text{O}$, 0.2420 g $\text{Na}_2\text{MoO}_4 \cdot 2\text{H}_2\text{O}$, 0 or 0.4656 g $\text{Co}(\text{NO}_3)_2 \cdot 6\text{H}_2\text{O}$, 1.7285 g $\text{Na}_4\text{P}_2\text{O}_7 \cdot 10\text{H}_2\text{O}$, 3.7385 g NaHCO_3 as the electroplate liquid was prepared. Finally, a two-electrode system is used for the electrodeposition of the NiMo/NF and NiMoCo/NF under a square-wave current-mode ($i_L = 0 \text{ mA cm}^{-2}$, $i_H = -150 \text{ mA cm}^{-2}$, the vacancy ratio of square waves is 0.5, the minimum period is 4 seconds) for 30 min. The Ni Foam (1*1 cm²) is used as the work electrode (WE) and a graphite plate (3*2 cm²) is used as the counter electrode (CE). After deposition, NiMoCo/NF were rinsed using DI water thoroughly and dried under nitrogen stream subsequently.

Synthesis of NiMoCo@CuS/NF: NiMoCo@CuS/NF was also synthesized through electrodeposition with two synthetic steps. Firstly, 50 mL ethanol solution containing 0.256 g $\text{CuCl}_2 \cdot 2\text{H}_2\text{O}$ as the electroplate liquid A was prepared. A two-electrode system is used for the electrodeposition of the NiMoCo@Cu/NF under a constant current mode ($i = -0.5 \text{ mA cm}^{-2}$) for 270 seconds. NiMoCo/NF (1*1 cm²) is used as WE and a graphite plate (3*2 cm²) is used as CE. After deposition, NiMoCo@Cu/NF is rinsed using ethanol thoroughly. Secondly, 50 mL ethanol solution containing Na_2S (supersaturation state) as the electroplate liquid B was prepared. A two-electrode system is also used for the electrodeposition of the amorphous NiMoCo@CuS/NF under a constant current mode ($i = 0.5 \text{ mA cm}^{-2}$) for 270 seconds.

NiMoCo@Cu/NF (1*1 cm²) is used as the WE and a carbon plate (3*2 cm²) is used as CE. After deposition, NiMoCo@CuS/NF is rinsed using ethanol thoroughly and dried under nitrogen stream subsequently.

Synthesis of CuS/NF: The synthesis process of CuS/NF is similar to that of NiMoCo@CuS/NF, except that NF was the WE.

Structure characterizations

The chemical composition was characterized with energy dispersive spectrometer (EDS) as shown in Figure S1. The purity was confirmed by X-ray photoelectron spectroscopy (XPS) with ESCALAB 250 Xi. X-ray diffraction (XRD) patterns were collected on a PANalytical X Pert Powder diffractometer with Ni K α radiation. The morphologies of the catalysts were observed using a field-emission scanning electron microscopy (SEM, Carry Scope JCM-5700) at accelerating voltage of 20 kV. The transmission electron microscopy (TEM) images were obtained on a JEM-2100HR, while Energy Dispersive X-Ray (EDX) mappings were acquired on an Oxford instrument IET250 spectrometer.

Electrochemical measurements

The electrocatalytic properties of the catalysts for HER were evaluated with a three-electrode system using a CHI electrochemical workstation (model 660E). The as-prepared composite was employed as the working electrode. A saturated calomel electrode (SCE) and a graphite plate were used as the reference and counter electrodes, respectively. All tests were carried out in solution of 0.5 M H₂SO₄. All potentials were measured relative to the reversible hydrogen electrode (RHE). Noted that the potential drop resulted from the ohmic loss on the electrolyte resistance has been subtracted. All potentials were referenced to the RHE through calibration: $E_{(RHE)} = E_{(SCE)} + 0.2415 + 0.059 \times \text{pH}$.¹ Linear sweep voltammetry (LSV) was conducted at a scan rate of 2 mV s⁻¹. Stability measurement was performed using chronopotentiometry, chronoamperometry, and accelerated degradation test (ADT). The ADT was performed by sweeping the potential in a range of 0 -120 mV versus RHE at a rate of 100 mV s⁻¹ with iR compensation of 90%. Electrochemical impedance spectroscopy (EIS) was

carried out in potentiostatic mode from 10^5 - 0.1 Hz with overpotential of 40 mV. All the polarization curves are recorded under a steady-state model after several cycles.

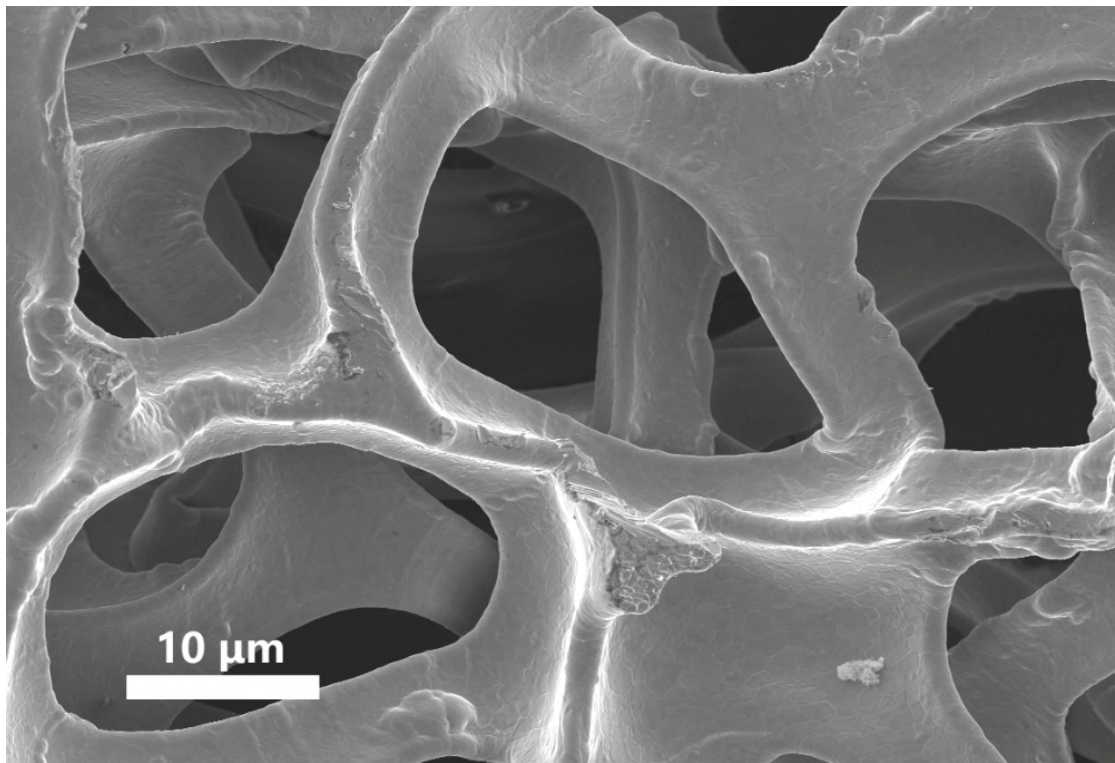


Figure S1. SEM image of NF.

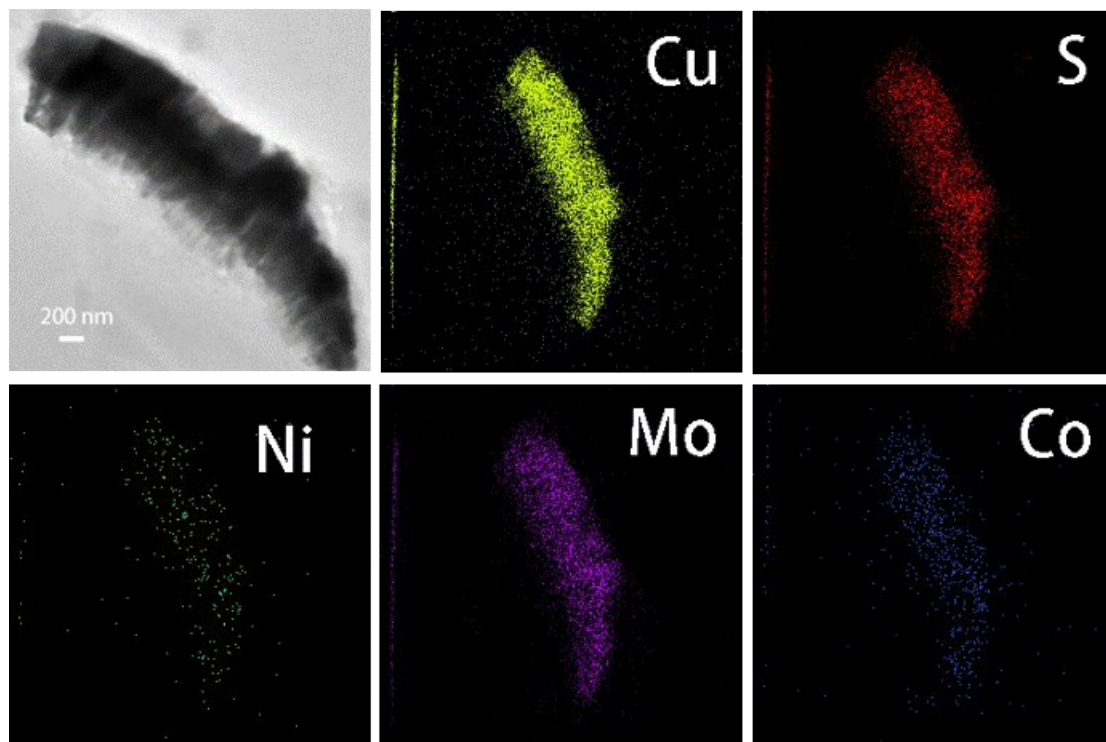


Figure S2. (a) TEM EDS image, (b) Cu, (c)S, (d) Ni, (e) Mo, and (f) Co mapping images of NiMoCo@CuS catalyst.

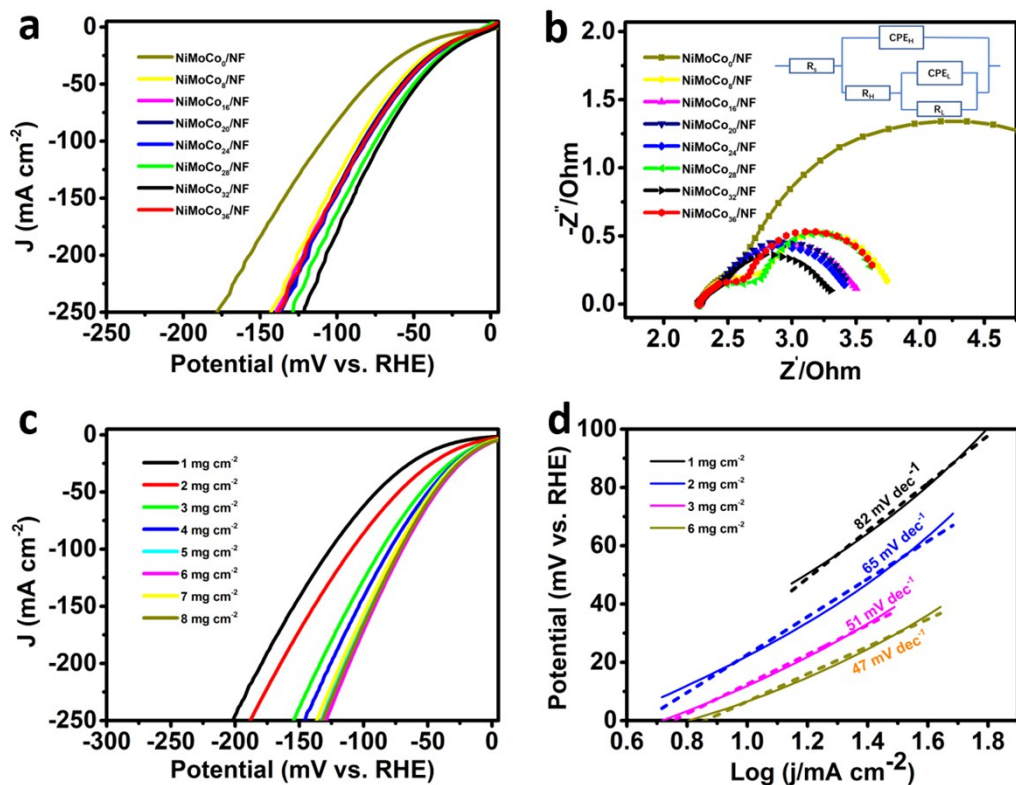


Figure S3. (a) Polarization curves ($iR=90\%$) of $\text{NiMoCo}_x/\text{NF}$ catalysts (scan rate 2 mV s^{-1} in $0.5 \text{ M H}_2\text{SO}_4$). (b) Nyquist plots for $\text{NiMoCo}_x/\text{NF}$ catalysts at a potential of 40 mV (vs. RHE). (c) Polarization curves ($iR=90\%$) of $\text{NiMoCo}_{32}/\text{NF}$ catalysts with different loading quantity (mg cm^{-2}). (d) Tafel plots.

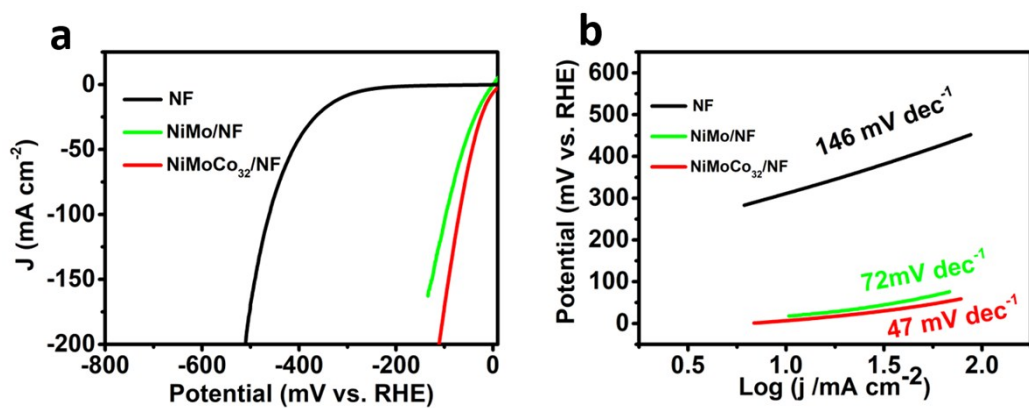


Figure S4. (a) Polarization curves and (b) the corresponding Tafel plots of NF, NiMo/NF and NiMoCo/NF at a scan rate of 2 mV s⁻¹ ($iR=90\%$).

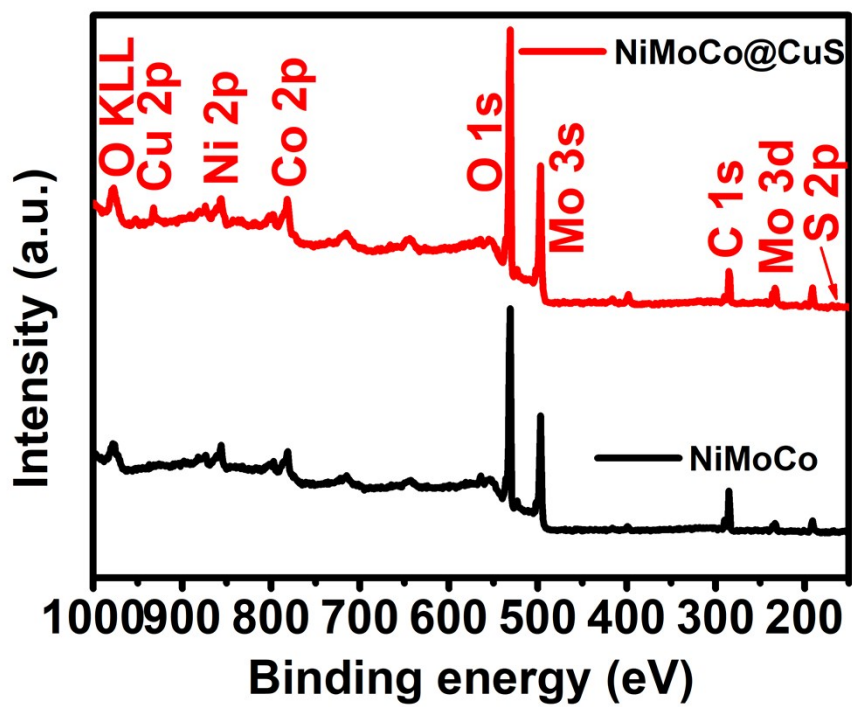


Figure S5. XPS full spectrum.

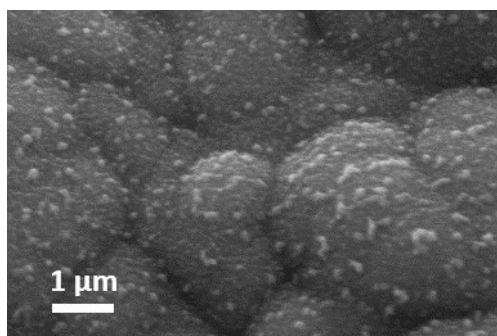


Figure S6. SEM images of NiMoCo@CuS/NF after stability test.

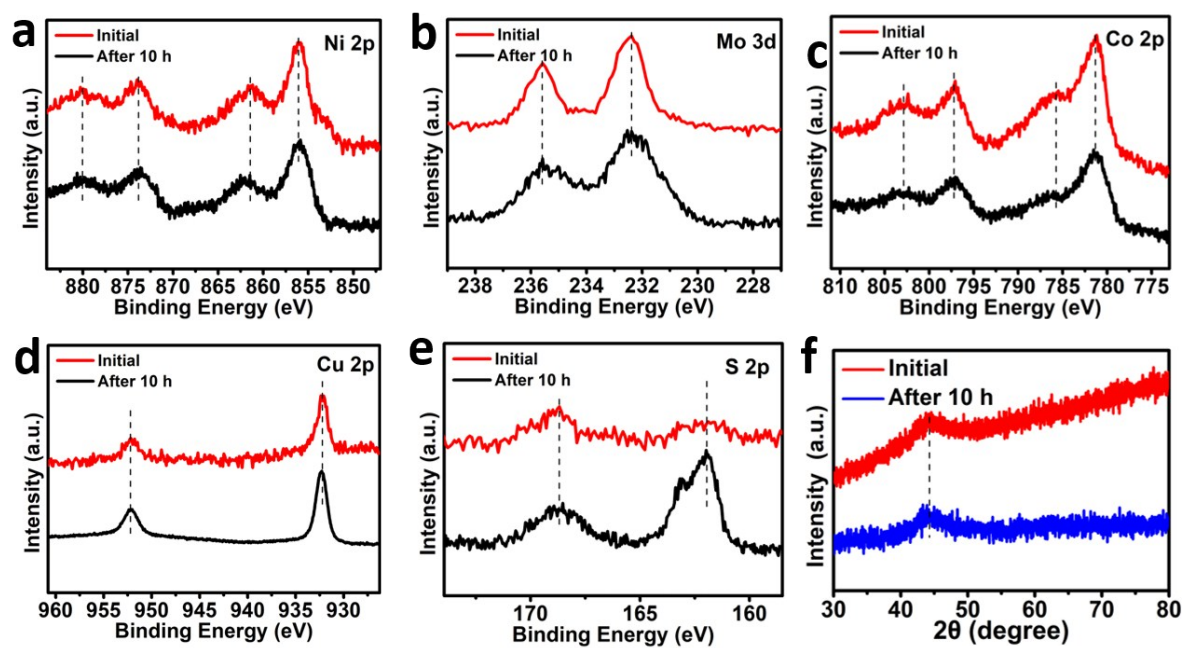


Figure S7. (a-e) XPS and (f) XRD of NiMoCo@CuS/NF before and after stability test.

Performance in alkaline solution:

In alkaline solution (1 M KOH), NiMoCo@CuS/NF (Figure S7a) shows an overpotential of 148 mV at current density of 100 mA cm^{-2} initially, which was then increased to 176 mV after stability test over 2h. And the time-dependent current density curve displays a drop of current density from 80 to 60 mA cm^{-2} within 2h. Comparing with the outstanding performance of NiMoCo@CuS/NF in acid solution (η_{100} @ 72 mV) as well as other efficient catalyst in alkaline solution,^{2,3} these results suggest that the NiMoCo@CuS/NF is not suitable for hydrogen electrochemical reaction in alkaline environment. Part of the reason may come from the electron withdrawing effect of S atom, leading to the poor efficiency of OH^- adsorption process.

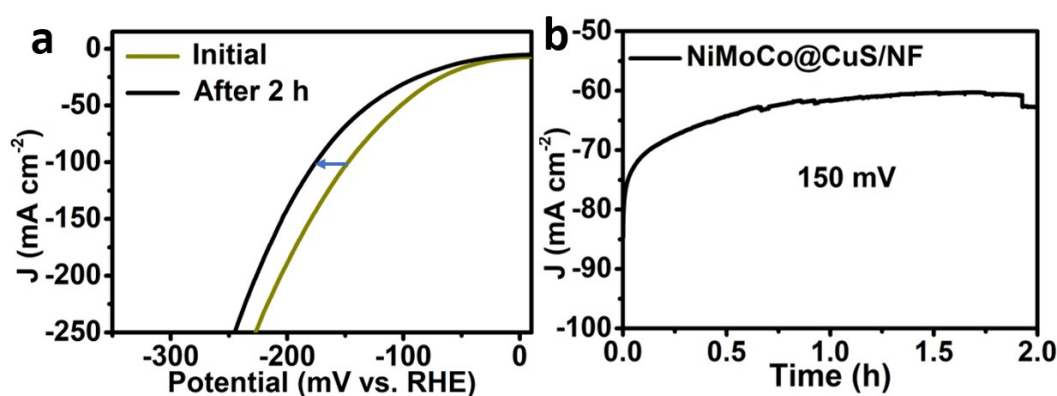


Figure S8. (a) Polarization curves ($iR = 90\%$) of NiMoCo@CuS/NF in 1 M KOH before and after 2h. (b) Time-dependent current density curve of NiMoCo@CuS/NF in 1 M KOH at an overpotential of 150 mV.

Influence of Cu on hydrogen evolution:

As shown in Figure S8, NiMoCo/NF and NiMoCo@Cu/NF display similar performance in 0.5 M H₂SO₄. The η_{100} of NiMoCo/NF and NiMoCo@Cu/NF equals to 73 mV and 76mV, respectively, suggesting that the deposition of Cu has limited influence on the hydrogen evolution efficiency.

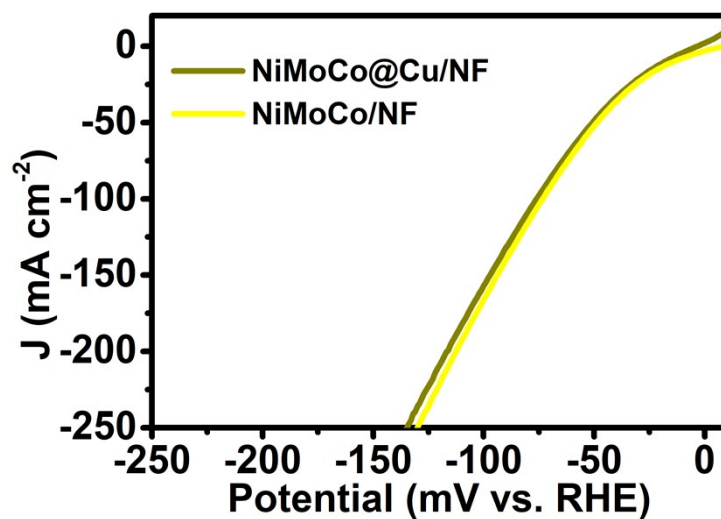


Figure S9. Polarization curves of NiMoCo/NF and NiMoCo@Cu/NF catalysts.

Table S1. Electroplating solution for synthesizing NiMoCo with the gradient concentration of cobalt. The concentrations of $\text{Na}_4\text{P}_2\text{O}_7$ and NaHCO_3 in the electroplating solution were 0.13 M and 0.89 M respectively for all samples.

	$\text{NiCl}_2 \cdot 6\text{H}_2\text{O}$ (mM)	$\text{Na}_2\text{MoO}_4 \cdot 2\text{H}_2\text{O}$ (mM)	$\text{Co}(\text{NO}_3)_2 \cdot 6\text{H}_2\text{O}$ (mM)
NiMoCo ₀	40	20	0
NiMoCo ₈	40	20	8
NiMoCo ₁₆	40	20	16
NiMoCo ₂₀	40	20	20
NiMoCo ₂₄	40	20	24
NiMoCo ₂₈	40	20	28
NiMoCo ₃₂	40	20	32
NiMoCo ₃₆	40	20	36

Table S2. The HER performance comparison

Note: All these data about HER activities are in geometric activities, calculated by dividing the current density per geometric area. All samples are tested in Electrolyte Solution of 0.5 M H₂SO₄.					
Catalyst	Current Density (J) (mA cm⁻²)	Overpotential at the corresponding J (mV vs. RHE)	Stability test (h)	Tafel (mV/dec)	Reference
NiMoCo@CuS/NF	10	14	~30	47	This work
	100	73			
Ni–Mo nanopowder	20	80	unstable	--	Reference ⁴
NiMoZn	20	46	--	--	Reference ⁵
	30	~50			
0.27Mo2.4Ni@900	10	75	2.8	128	Reference ⁶
Ni/Co-S	10	85	12	61	Reference ⁷
	100	182			
NiCoS _{0.14} O _{3.25} NSs/NF	10	170	18	94.3	Reference ⁸
Ni–Co–MoS ₂	10	155	--	51	Reference ⁹
NiMoN _x /C	2	170	--	35.9	Reference ¹⁰
CFP/NiCo ₂ O ₄ /CuS	10	72.3	50	41	Reference ¹¹
MoS ₂ /CuS	10	290	6.6	30	Reference ¹
Co _{0.1} Ni _{0.75} Se/rGO	10	103	30	43	Reference ¹²
Ni(OH) ₂ @CuS	10	95	30	104	Reference ¹³
Ni ₂ P/Ni	20	~150	65	68	Reference ¹⁴
Ni _x P _y -325	20	62	18	46.1	Reference ¹⁵
NiSe ₂ /Ni	10	143	18	49	Reference ¹⁶

Table S3. Z-fit equivalent circuit data at -40 mV (vs. RHE) of NiMoCo_x

Sample	R _H	CPE _H -P	R _L	CPE _L -P	τ _H (s)	τ _L (s)
NiMoCo ₀	0.47	0.90	3.15	0.87	0.42	2.74
NiMoCo ₈	0.47	0.90	1.00	0.95	0.42	0.95
NiMoCo ₁₆	0.35	0.80	0.87	0.95	0.28	0.83
NiMoCo ₂₀	0.35	0.80	0.81	0.95	0.28	0.77
NiMoCo ₂₄	0.31	0.80	0.80	0.95	0.25	0.76
NiMoCo ₂₈	0.4	0.78	0.80	0.95	0.31	0.76
NiMoCo ₃₂	0.34	0.80	0.65	0.95	0.27	0.62
NiMoCo ₃₆	0.47	0.79	0.95	1.05	0.37	1.00

Reference

- 1 L. Zhang, Y. Guo, A. Iqbal, B. Li, D. Gong, W. Liu, K. Iqbal, W. Liu and W. Qin, *International Journal of Hydrogen Energy*, 2018, **43**, 1251–1260.
- 2 J. Zhang, T. Wang, P. Liu, Z. Liao, S. Liu, X. Zhuang, M. Chen, E. Zschech and X. Feng, *Nature Communications*, 2017, **8**, 1–8.
- 3 Z. Y. Yu, Y. Duan, M. R. Gao, C. C. Lang, Y. R. Zheng and S. H. Yu, *Chemical Science*, 2017, **8**, 968–973.
- 4 J. R. McKone, B. F. Sadtler, C. A. Werlang, N. S. Lewis and H. B. Gray, *ACS Catalysis*, 2013, **3**, 166–169.
- 5 X. Wang, R. Su, H. Aslan, J. Kibsgaard, S. Wendt, L. Meng, M. Dong, Y. Huang and F. Besenbacher, *Nano Energy*, 2015, **12**, 9–18.
- 6 S. Wang, J. Wang, M. Zhu, X. Bao, B. Xiao, D. Su, H. Li and Y. Wang, *Journal of the American Chemical Society*, 2015, **137**, 15753–15759.
- 7 Z. Ma, Q. Zhao, J. Li, B. Tang, Z. Zhang and X. Wang, *Electrochimica Acta*, 2018, **260**, 82–91.
- 8 C. Li, X. Zhao, Y. Liu, W. Wei and Y. Lin, *Electrochimica Acta*, 2018, **292**, 347–356.
- 9 X. Y. Yu, Y. Feng, Y. Jeon, B. Guan, X. W. D. Lou and U. Paik, *Advanced Materials*, 2016, **28**, 9006–9011.
- 10 W. F. Chen, K. Sasaki, C. Ma, A. I. Frenkel, N. Marinkovic, J. T. Muckerman, Y. Zhu and R. R. Adzic, *Angewandte Chemie - International Edition*, 2012, **51**, 6131–6135.
- 11 L. An, L. Huang, P. Zhou, J. Yin, H. Liu and P. Xi, *Advanced Functional Materials*, 2015, **25**, 6814–6822.
- 12 W. Zhao, S. Wang, C. Feng, H. Wu, L. Zhang and J. Zhang, *ACS Applied Materials and Interfaces*, 2018, **10**, 40491–40499.
- 13 S. Q. Liu, H. R. Wen, Ying-Guo, Y. W. Zhu, X. Z. Fu, R. Sun and C. P. Wong,

- Nano Energy*, 2018, **44**, 7–14.
- 14 Y. Shi, Y. Xu, S. Zhuo, J. Zhang and B. Zhang, *ACS Applied Materials and Interfaces*, 2015, **7**, 2376–2384.
- 15 J. Li, J. Li, X. Zhou, Z. Xia, W. Gao, Y. Ma and Y. Qu, *ACS Applied Materials and Interfaces*, 2016, **8**, 10826–10834.
- 16 H. Zhou, Y. Wang, R. He, F. Yu, J. Sun, F. Wang, Y. Lan, Z. Ren and S. Chen, *Nano Energy*, 2016, **20**, 29–36.